Mechanisms of xylem hydraulic recovery after drought in *Eucalyptus saligna*

Alice Gauthey[1], Jennifer M. R. Peters[1,2], Rosana Lòpez[1,3], Madeline R. Carins-Murphy[4], Celia M. Rodriguez-Dominguez[5], David T. Tissue[1], Belinda E. Medlyn[1], Tim J. Brodribb[4], Brendan Choat[1]

1. *Western Sydney University, Hawkesbury Institute for the Environment, Richmond, NSW 2753, Australia*
2. *Oak Ridge National Laboratory, Climate Change Science Institute & Environmental Science Division, Oak Ridge, TN USA*
3. *Departamento de Sistemas y Recursos Naturales, Universidad Politécnica de Madrid, Madrid, Spain*
4. *School of Biological Sciences, University of Tasmania, Private Bag 55, Hobart, Tasmania 7001, Australia*
5. *Irrigation and Crop Ecophysiology Group, Instituto de Recursos Naturales y Agrobiología de Sevilla (IRNAS, CSIC), Avenida Reina Mercedes,10, Sevilla 41012, Spain*

Running head: Xylem hydraulic recovery after drought

Funding information

This research was supported by an ARC Future Fellowship to BC (FT130101115), an ARC Discovery proposal to TJB and BC (DP170100761), and Marie Skłodowska-Curie grants to RL (FP7-PEOPLE-2013-IOF-624473) and CMRD (751918-AgroPHYS). MicroCT imaging and image analysis was facilitated by beamtime allocations from the Australian Synchrotron to BC (projects 12579, 13106).

Author for correspondence: Brendan Choat

Email: b.choat@westernsydney.edu.au

Phone: +61 2 4751 1901

ABSTRACT

The mechanisms by which woody plants recover xylem hydraulic capacity after drought stress are not well understood, particularly with regard to the role of embolism refilling. We evaluated the recovery of xylem hydraulic capacity in young *Eucalyptus saligna* plants exposed to cycles of drought stress and rewatering. Plants were exposed to moderate and severe drought stress treatments, with recovery monitored at time intervals from 24 hrs to 6 months after rewatering. The percentage loss of xylem vessels due to embolism (PLV) was quantified at each time point using micro-computed tomography with stem water potential (Ψ_x) and whole plant transpiration (E_{plant}) measured prior to scans. Plants exposed to severe drought stress suffered high levels of embolism (47.38 ± 10.97 % PLV) and almost complete canopy loss. No evidence of embolism refilling was observed at 24 hrs, one week, or three weeks after rewatering despite rapid recovery in Ψ_x. Recovery of hydraulic capacity was achieved over a 6-month period by growth of new xylem tissue, with canopy leaf area and E_{plant} recovering over the same period. These findings indicate that *E. saligna* recovers slowly from severe drought stress, with potential for embolism to persist in the xylem for many months after rainfall.

Keywords: xylem, drought, water-stress, hydraulic, embolism, cavitation, refilling, recovery, microCT, water potential.

INTRODUCTION

Water is transported through the xylem as a liquid under tension (Tyree and Ewers, 1991; Tyree, 1997; Steudle, 2001). In this physical state, water may undergo cavitation, resulting in the formation of gas emboli and blockage of xylem conduits. Water stress causes tension in the xylem to increase, which leads to a higher probability of cavitation. Although the structure of the xylem has evolved to limit the impact of embolism, at a critical tension, embolism will begin to spread rapidly through the network of conduits, leading to a sharp decrease in xylem hydraulic conductivity (Brodersen, 2013; Lens et al., 2013; Knipfer et al., 2015b). As a consequence, the capacity of plants to move water from the roots to the leaves is reduced, affecting leaf gas exchange and tissue hydration (Nardini et al., 2003; Martorell et al., 2014; Knipfer et al., 2015b). During periods of severe water stress, embolism can lead to complete hydraulic failure in roots, stems and leaves, which has been linked to canopy dieback and whole plant mortality during drought.

Plants have developed a range of strategies to survive and recover from water stress, which include avoidance of water stress by stomatal regulation, leaf shedding, and access to ground water (Čermák et al., 1980; Molyneux and Davies, 1983; Robichaux et al., 1987; Cochard et al., 1996; David et al., 2013), and tolerance of water stress due to high resistance to cavitation, low turgor loss points and wider hydraulic safety margins (Choat et al., 2012). However, regardless of strategy, when the xylem tension reaches critical thresholds set by cavitation resistance, blockage of xylem conduits by embolism will progressively reduce xylem hydraulic conductivity. Physiological mechanisms that restore xylem hydraulic capacity are a key component of recovery from drought stress.

A large body of research has focused on mechanisms that allow plants to refill embolized xylem conduits on short time scales (ca. 6-12 hrs), thus providing rapid recovery of hydraulic capacity after drought. The process of embolism repair (i.e. refilling) requires a mechanism by which gas is reabsorbed into the water and removed from xylem conduits. The exact physiological mechanisms responsible for refilling, and the prevalence of embolism repair across plant taxa, are issues that have been widely debated over the last 40 years (Sperry et al., 1988; Borghetti et al., 1991; Salleo et al., 1996; Tyree et al., 1999; Holbrook et al., 2001; Salleo et al., 2009; Zwieniecki and Holbrook, 2009; Brodersen et al., 2010; Brodersen and McElrone, 2013). Pickard (1989) hypothesised that root pressure could dissolve gas bubbles during the night-time when transpiration was minimal and soil water availability was high. Springtime refilling is

commonly observed in some plant species exposed to freezing conditions during winter, including vines and tree species that are known to generate strong positive root and stem pressures (Sperry et al., 1987; Pockman and Sperry, 1997; Utsumi et al., 1998; Ewers et al., 2001; Cobb et al., 2007; Christensen-Dalsgaard and Tyree, 2014; Mayr et al., 2014). It is important to note that such springtime refilling is an adaptation to embolism caused by successive freeze-thaw cycles during winter and occurs in concert with major remobilisation of water and carbohydrate reserves after winter dormancy (Charrier et al., 2013; Mayr et al., 2014; Plavcová and Jansen, 2015). It is therefore distinct in a number of important ways from the proposed diurnal refilling process or refilling after drought stress during the growing season (Klein et al., 2018).

Without conditions creating positive pressures throughout the xylem, refilling is difficult to explain in terms consistent with the laws of thermodynamics (Holbrook and Zwieniecki, 1999; Zwieniecki and Holbrook, 2009). However, several studies have concluded that refilling under tension is possible and could occur as part of a diurnal cycle in certain species (*Vitis vinifera*, Jacobsen & Pratt, 2012; *Quercus gambelii,* Taneda and Sperry, 2008). A number of theories have been advanced to explain refilling under tension, with most centring on osmotic activity of xylem parenchyma cells adjacent to embolised conduits and the isolation of refilling conduits from the transpiration stream (Clearwater and Goldstein, 2005; Salleo et al., 2009; Zwieniecki and Holbrook, 2009; Nardini et al., 2011; Brodersen and McElrone, 2013). Observations suggest that refilling takes place over a period of hours, allowing restoration of xylem function within relatively short time periods (Nardini et al., 2011). An alternative mechanism of recovery is the growth of new xylem tissue. In this case, recovery of hydraulic capacity would occur over much longer time frames (weeks, months) and require significantly more investment of carbon. In conifer species, two studies have demonstrated that recovery of hydraulic capacity after severe drought stress is facilitated by growth of new xylem tissue rather than refilling of embolised tracheids (Brodribb et al., 2010; Hammond et al., 2019; Secchi et al., 2020).

The application of non-invasive imaging techniques allowed researchers to visualise refilling in intact plants, including observations based on Magnetic Resonance Imaging (MRI) and micro computed tomography (microCT) (Brodersen et al., 2010; Ryu et al., 2016; Gleason et al., 2017; Secchi et al., 2020). These studies have provided evidence of embolism repair in a limited number of species (grapevine, maize, poplar) capable of producing strong root pressure (Charrier et al., 2016). However, other studies using MRI and microCT have provided evidence

that refilling does not occur after drought, despite water potentials recovering to pre-drought levels on short time scales (Clearwater and Clark, 2003; Brodribb et al., 2010; Choat et al., 2015; Knipfer et al., 2015b; Choat et al., 2018; Johnson et al., 2018). Additionally, there is evidence that observations of refilling based on hydraulic (flow-based) measurements may be flawed because of experimental artefacts relating to excision of samples under tension (Wheeler et al., 2013; Torres-Ruiz et al., 2015; Lamarque et al., 2018). This work has raised questions regarding the generality of embolism repair mechanisms across plant taxa and the processes that plants use to recover hydraulic capacity in the absence of refilling.

In this study, we used microCT visualisation to investigate whether refilling is a routine mechanism of recovery from drought stress in the evergreen tree species, *Eucalyptus saligna*. In a recent study utilising microCT, we observed partial refilling in a small fraction of embolised vessels in *Eucalyptus saligna* plants recovering from drought stress, although this did not result in a significant decrease in the number of embolised vessels over all (Choat et al., 2019). However, two studies have also suggested that X-ray damage caused by microCT scans may impact xylem physiological function, including mechanisms of embolism refilling that rely on the metabolic activity of living cells in the xylem (Savi et al., 2017; Petruzzellis et al., 2018). In order to address this issue and avoid artefacts associated with X-ray damage, data in the current study were acquired from single scans of multiple replicate plants, rather than repeated scans on individual plants. Recovery of hydraulic capacity, plant water status, and canopy transpiration rates were evaluated in plants exposed to moderate drought (MD) and severe drought (SD) stress over time scales ranging from 24 hrs to 6 months. Monitoring recovery over longer time periods allowed us to examine embolism refilling and growth of new xylem tissue as alternative mechanisms of recovery.

MATERIALS AND METHODS

Plant material

Eucalyptus saligna Sm. (Sydney Blue Gum) is fast growing tree species used extensively in timber plantations. It is native to mesic areas along the eastern coast of Australia in New South Wales and Queensland and is relatively vulnerable to drought compared to other *Eucalyptus* species (Bourne et al., 2017). Thirty-three plants were purchased from PlantPlus Cumberland forest nursery (Pennant Hills, NSW, Australia). Plants were grown in 4-L plastic pots using standard potting mix and were kept in a sunlit poly-tunnel on the Hawkesbury Campus of Western Sydney University (Richmond, NSW, Australia) for three weeks. Plants were

approximately 1-year-old and 1 metre in height at the beginning of the experiment. The experiment commenced in September 2017 and finished in March 2018.

Drought treatment

A first subset of plants was allocated to two different treatments: (1) medium drought (MD) (n=5) in which plants were dried to a water potential target of ~ -2 MPa and then rewatered, and (2) severe drought (SD) (n=9) in which plants were dried to a water potential target of ~ -3.5 MPa and then rewatered (Fig. S1). These water potential targets were based on previous studies (Bourne et al., 2017; Choat et al., 2019) and were expected to induce complete stomatal closure and a given percentage of loss of conductivity (PLC) of ~10% in MD and ~50% PLC in SD. Whole canopy transpiration rate (E_{plant}) and stem water potential (Ψ_x) were tracked during the dry-down and the recovery for these two treatments. The two drought treatments allowed us to assess recovery of leaf gas exchange as a function of the severity of the water stress (minimum water potential reached) and the impact on theoretical hydraulic conductivity. All plants were kept in a sunlit polytunnel for three weeks prior to the start of drought treatments. In order to impose uniform conditions during the application of drought treatments, individuals assigned to MD and SD treatments were moved to a controlled environment chamber (Thermoline, Australia) maintained at 21°C constant temperature with a 11h/13h light/dark cycle with a photon flux density of 700 μmol m^{-2} s^{-1} and 60% relative humidity. Water was withheld from plants until the desired Ψ_x for each treatment was reached. At this point, plants were moved to a second growth chamber and E_{plant} was measured (see details below). Plants were returned to the poly-tunnel during the recovery phase and watered daily to maintain high plant and soil water status.

In order to address issues regarding the impacts of X-ray radiation on xylem physiological processes raised in recent studies (Savi et al., 2017; Petruzzellis et al., 2018), the majority of plants included in this experiment were scanned only once. In this experimental design, changes in the number of embolised vessels at different time points were measured on separate cohorts of individuals, rather than by repeated measurements on individual plants. While this approach does not allow changes in the status of individual vessels to be tracked, it avoids any potential impacts of X-ray radiation on the activity of living parenchyma cells within the xylem, which theoretically drive embolism refilling. As such, a second subset of plants (n=19) was assigned to allow for micro-CT visualisation of xylem tissue at different points during drought and

recovery treatments. Groups of plants scanned in this manner were assigned to well-watered (n=4), dried to MD (n=5), dried to SD (n=5), and dried to MD and rewatered 24 hours (R24h) before scanning (n=5). After initial scans, the well-watered group of plants was scanned three further times to allow for construction of a dehydration vulnerability curve for which plants were dehydrated down to ~-2.8 MPa (see below). Previous work has demonstrated that multiple scans on individual plants do not alter vulnerability curves (Choat et al., 2016; Gauthey et al., 2020). Canopy transpiration rates and water potential were recorded for each replicate plant immediately before microCT scans took place in both subset of plants. In order to track long-term recovery from drought, SD individuals from the first plant subset were scanned after three weeks (R3wk) (n=5) and six months (R6mo) of recovery (n=4) after rewatering (Fig. S1).

Physiological and morphological measurements

Bagged leaf (stem) water potential (Ψ_x) was measured by sealing a leaf in plastic film, covered in aluminium foil, for a minimum of 30 min before excision and measurement (McCutchan and Shackel, 1992; Choat et al., 2010). Leaves were slowly (0.02 MPa s^{-1}) and continuously pressurized with a Scholander pressure chamber (PMS Instrument Company, Albany, OR, USA) until water was visible on the cut end of the leaf (Scholander et al., 1965). Two to three leaves (or small branch tips when leaves became too dry) per individual were measured for each water potential measurement. When Ψ_x could not be measured using the pressure chamber method because of canopy leaf loss, Ψ_x was assessed using PSY1 Stem Psychrometer sensor coupled with a microvolt data logger used to store data **(**ICT International, Armidale, NSW, Australia).

A second growth-chamber was used to measure canopy transpiration rate (E_{plant}) throughout the experiment. The chamber environmental conditions were maintained at 25°C, constant light intensity of 700 μmol m^{-2} s^{-1} and 60% relative humidity during measurement periods. Plants were placed on a precision balance with a resolution of 0.1g (MS8001TS, Mettler-Toledo, Columbus, OH, USA) connected to a data logger (CR1000, Campbell Scientific, UT, USA). Changes in weight were recorded with LoggerNet software (Campbell Scientific, UT, USA). Prior to measurements, a plastic bag was sealed around the pots to cover the soil and minimise soil evaporation. Weight was logged from the balance every minute for a 1 to 2 hr period per plant with differences in weight attributed to plant water loss. Whole canopy transpiration rate (g $plant^{-1}$ hr^{-1}) was calculated as the slope of a linear regression between plant water loss and

time. Throughout the experiment, the canopy leaf area was recorded by counting the number of mature leaves on each plant. A relationship between leaf number, weight and area was established to allow calculation of total canopy leaf area at each time point.

MicroCT scans

MicroCT visualisations were undertaken at the Australian Synchrotron (Clayton, VIC, Australia) Imaging and Medical Beamline (IMBL) during two periods: late October of 2017 and early March of 2018. Samples were positioned in the beam using a robotic arm (Kuka, KR1000 Titan) and scanned at the main stem axis with a field of view of 28 mm x 20 mm. Scans were conducted at an X-ray energy of 30 keV, while the sample was rotated through 180 degrees using continuous rotation; images were recorded at 0.1° angle increments. This yielded 1800 projections with additional flat-field and dark-field images recorded before and after each scan. Exposure time at each angle was 0.45–0.60 s giving a total scan time of 18–23 min. Scan volumes were reconstructed using XLICT Workflow 2015 (CSIRO) using either the Gridrec or FBP (Paganin et al., 2002) reconstruction algorithm. The final resolution of images was 9.7 μm per voxel. MicroCT images provided good contrast between water-filled (grey) and air-filled (black) vessels. Image analysis was performed on a median scan (10 middle scans were compressed to make a single scan) by counting embolised vessels (darker than water-filled ones) using the 'Threshold' and 'Analyse Particles' functions in ImageJ, or by counting vessels manually using the "multi-point" action (Nolf et al., 2017). Percentage of loss of vessels (PLV) was calculated for each scan image following:

$$PLV = \frac{Number\ of\ vessels\ embolised}{Total\ number\ of\ vessels} \times 100$$

The strong correlation between PLV and PLC is supported by numerous studies (Gauthey et al., 2020; Li et al., 2020; Peters et al., 2020) which suggests that loss of conductivity in this species can be approximated by counting gas filled vessels, especially for species with diffuse porous xylem structure, in which the distribution of vessel diameters is relatively narrow.

In order to estimate what percentage of new xylem was regrown after rewatering, we used cross-sections of the 6-month recovery plants to analyse the area of xylem occupied by newly grown xylem or older xylem. Images were processed with ImageJ where pit and bark were removed, and old and new xylem area were calculated.

Vulnerability curves

Two vulnerability curves (VCs) were generated using PLV and Ψ_x measurements from all plants in drought and recovery treatments (n=26). The first VC was fitted to data from plants that were scanned during the dehydration phase (VC_D, dehydration curve). To further examine evidence of refilling, we plotted the PLV of recovery treatment plants against the minimum water potential that they experienced during drought. These rehydration points were also transposed to the minimum Ψ_x that the plant reached before rewatering, and a second curve (VC_R) was fitted to these data (transposition curve).

Statistical analysis

All statistical analyses were conducted with R 3.1.2 (R Core Team, 2017) using RStudio (RStudio Team, 2015). Comparison of the physiological and morphological traits between the two treatments were tested for significant differences with a one-way ANOVA. Analyses were conducted on untransformed data which were normally distributed. Vulnerability curves were fit to PLV using the *fitplc* package following methods developed by Duursma & Choat (2017). Curves were fit with a Weibull function and the mean P_{50} and confidence intervals were extracted using a standard profiling method. For these methods, a 95% CI for the estimate of P_{50} was generated using a bootstrapping approach with 2000 resamples. To test for significant differences between vulnerability curves (dehydration and transposition), we generated bootstrap confidence intervals (CIs) for the difference in estimates of P_{50} for each dataset (Gauthey et al., 2020).

RESULTS

Dynamics of transpiration and plant water status

At the commencement of the experiment, plants allocated to SD treatment had high mean stem water potential (Ψ_x = -0.44 ± 0.02 MPa) and a mean E_{plant} of 48.3 ± 2.6 g plant^{-1} hr^{-1} (Fig. 1). As SD plants were dehydrated to a mean Ψ_x of -2.11 ± 0.21 MPa, stomata closed and E_{plant} was sharply reduced to 15.7 ± 3.0 g plant^{-1} hr^{-1}. When plants reached the severe drought target water potential (Ψ_x = -3.17 ± 0.17 MPa), E_{plant} was further reduced to 1.9 ± 0.2 g plant^{-1} hr^{-1}. At this time point, leaves on all plants in the SD treatment had become severely wilted. Upon release from drought, stem water status slowly recovered to Ψ_x = -2.10 ± 0.33 MPa at 24 hr after rewatering and to Ψ_x = -1.34 ± 0.42 MPa at 1 week after rewatering. During this time, the majority of plants in the SD treatment experienced complete canopy loss (100% leaf death) and

E_{plant} remained stable at 1.3 ± 0.3 g plant^{-1} hr^{-1}. By 3 weeks after rewatering, Ψ_x had recovered to -0.37 ± 0.07 MPa, excluding one individual that did not recover after rewatering (Ψ_x = -5.00 MPa). At 3 weeks post drought, two plants had recovered a small proportion (~30%) of their initial canopy area, while most other individuals were in the initial phases of resprouting from epicormic buds; mean E_{plant} remained low at 3.0 ± 1.7 g plant^{-1} hr^{-1}. Over the longer term, plants from the SD treatment fully recovered water status, canopy leaf area, and transpiration rate; at 18 weeks post-drought, mean Ψ_x = -0.58 ± 0.08 MPa and mean E_{plant} = 44.9 ± 7.5 g plant^{-1} hr^{-1}. In all long-term recovery plants, some proportion of the main stem axis died, and recovery of leaf area occurred from growth of new branches and epicormic buds. After 6 months under well-watered conditions, plants had 1.3 to 2.4 fold higher canopy leaf area and significantly higher canopy transpiration rates (E_{plant} = 78.9 ± 5.29 g plant^{-1} hr^{-1}) than at the time of initial measurements, while plant water status remained high (Ψ_x = -0.56 ± 0.04 MPa) (Fig. 1B and D). When transpiration rate was expressed on a leaf area basis (E_c), it was slightly, although not significantly, lower than at the initial measurement point (Fig. S2).

In the MD treatment, stomatal closure reduced E_{plant} from an initial rate of 103.6 ± 3.6 g plant^{-1} hr^{-1} to 10.2 ± 0.4 g plant^{-1} hr^{-1} at the peak of the drought treatment (Ψ_x = -1.94 ± 0.14 MPa) (Fig. 1A and C). No canopy loss and only mild wilting was observed at the peak of this moderate drought stress treatment. At 24 hrs after rewatering, MD plants had recovered close to their initial pre-treatment water status (Ψ_x = -0.90 ± 0.20 MPa), while E_{plant} had recovered to approximately half of initial values (55.8 ± 2.9 g plant^{-1} hr^{-1}) in all but one individual, for which E_{plant} was 3.9 g plant^{-1} hr^{-1}. Mean E_{plant} remained unchanged 5 days after rewatering, at 52.7 ± 1.6 g plant^{-1} hr^{-1} for four individuals and 5.0 g hr^{-1} for one outlier. At 1 week after rewatering, two individuals experienced approximately 90% loss of canopy leaf area, leading to sharply lower E_{plant} (3.7 ± 2.2 g plant^{-1} hr^{-1}) for these two individuals compared to a mean E_{plant} of 45.9 ± 1.2 g plant^{-1} hr^{-1} for the three individuals that retained their full canopies. At 2 weeks after rewatering, the three plants with canopy remaining had a mean E_{plant} of 48.9 ± 11.4 g plant^{-1} hr^{-1} and mean Ψ_x of -0.78 ± 0.07 MPa (Fig. 1A and C). Transpiration rate on a leaf area basis (E_c) agreed with these E_{plant} dynamics (Fig. S2).

Refilling observation

Well-watered plants exhibited low levels of native embolism (Figs. 2 and 3). In the SD treatment, PLV increased to 47.4 ± 11 % at the peak of the drought (Ψ_x = -3.26 ± 0.15 MPa).

After rewatering in the SD treatment, the lack of transpiration due to leaf shedding and well-watered soil were expected to provide favourable conditions for refilling. However, at 3 weeks after rewatering, mean PLV was 64.7 ± 18.7 %, higher than PLV recorded for SD plants at the peak of drought stress. After six months under well-watered conditions, plants exposed to severe drought treatment retained very high levels of embolism in xylem that had been exposed to the severe drought treatment (Fig. 2B). New xylem growth with relatively few embolised vessels surrounded the core of embolised vessels in the old xylem (Fig. 4). MicroCT visualisation allowed us to quantify the level of embolism in the old xylem and the new xylem grown during the 6 months recovery period. This analysis yielded a mean PLV of 8.0 ± 3.0 % for the new ring and mean PLV of 47.2 ± 5.1 % for the whole stem cross section (Fig. 2B).

MicroCT visualisations indicated that the MD treatment (Ψ_x = -1.98 ± 0.17 MPa) resulted in a small increase in the number of embolised vessels (PLV of 7.8 ± 1.8 %), although this was not significantly different from native embolism observed in well-watered plants (PLV of 3.6 ± 1.2 %). In samples exposed to a MD treatment (Ψ_x = -2.02 ± 0.21 MPa) and then allowed to recover for 24 hours, the PLV was 4.9 ± 1.8 %, which was not significantly different from PLV observed for the MD treatment. However, in plants allowed to recover for one week after MD, the number of embolised vessels was higher (PLV = 24.6 ± 9.0 %) than that observed for MD or 24 hours recovery treatments (Fig. 2A). It is notable that this increase was primarily due to higher PLV in two individuals, which were also the only plants to suffer significant canopy leaf loss as a result of the MD treatment (see above). The occurrence of higher PLV in plants that had been recovering from MD or SD treatments for 1 week and 3 weeks, respectively, was an unexpected result that could not be explained by differences in the minimum water potential reached in different treatments.

No evidence of embolism repair was observed in microCT scans during the recovery period, regardless of drought stress intensity (MD or SD) or the time length of recovery (Fig. 2). Where recovery in hydraulic capacity did occur, it was over longer time frames (6 months) and was due to growth of new xylem tissue rather than embolism repair (Figs. 4 and 5).

Vulnerability curves

The vulnerability curve based on dehydrated plants (VC_D) indicated that *E. saligna* saplings were sensitive to drought relative to other *Eucalyptus* species, with P_{50} = -3.3 MPa (Fig. 6). We predicted that if the vulnerability curve based on the minimum water potential reached by

recovery plants (VC_R) and VC_D were similar, then xylem refilling was unlikely to have occurred. For the VC_R curve, P_{50} = -3.1 MPa, which was not significantly different from the P_{50} estimated from the VC_D. This provides evidence that embolism which occurred as a result of drought stress treatments was preserved in the xylem even after rewatering for a number of weeks.

DISCUSSION

Recovery of xylem hydraulic capacity following severe water stress and high levels of xylem embolism was facilitated by growth of new xylem rather than embolism refilling in a woody angiosperm species, *Eucalyptus saligna*. Despite recovery of plant water potential after irrigation, microCT observations of embolism in the stem xylem revealed no evidence of embolism repair between 24 hrs and 3 weeks after water stress was relieved. Over longer time periods (6 months), plants recovered xylem hydraulic capacity by growing new xylem, while the older xylem remained embolised and non-functional. Whole plant transpiration rates recovered over this time period in proportion to re-expansion of canopy leaf area following rewatering. In plants that were subjected to moderate water stress, reductions in whole plant transpiration were observed, indicating stomatal closure, but there was no significant increase in mean PLV relative to pre-drought values. Plant water status and whole plant transpiration recovered rapidly after irrigation in the majority of MD plants, with individuals that suffered higher levels of embolism exhibiting more limited recovery. Despite numerous studies suggesting that refilling can occur under low tensions in the xylem, we did not observe embolism repair in MD or SD treatments, even when stem water potentials recovered to high values (> -0.5 MPa). These results provide further evidence that embolism refilling may not be a widespread mechanism of hydraulic recovery in woody plants following drought stress events.

Previous experimental work provides contrasting evidence regarding the extent of embolism repair during recovery from drought. While some studies suggest that refilling is a routine process that occurs on diurnal timescales (Canny, 1997), or if the xylem is under mild tension (Holbrook et al., 2001; Hacke and Sperry, 2003; Brodersen et al., 2010; Yang et al., 2012), other studies indicate that refilling does not play a major role in the recovery of xylem hydraulic capacity after drought (Clearwater and Clark, 2003; Brodribb et al., 2010; Choat et al., 2015; Knipfer et al., 2015b; Choat et al., 2019; Hammond et al., 2019). Similarly, our micro-CT observations demonstrated that embolism repair did not occur in *E. saligna*, regardless of water

388 stress intensity or time period after rewatering (Figs. 2 and 3). The introduction of non-invasive
389 imaging techniques has provided opportunities to examine the refilling process in
390 unprecedented spatial and temporal detail, while avoiding artefacts associated with destructive
391 sampling (Holbrook et al., 2001; Brodersen et al., 2010). However, a number of studies that
392 utilize non-invasive imaging techniques have shown limited evidence of refilling after drought
393 in angiosperm and gymnosperm species (Choat et al., 2015; Knipfer et al., 2015b; Choat et al.,
394 2018; Lamarque et al., 2018; Rehschuh et al., 2020).
395
396 While non-invasive methods have many advantages in the study of xylem function, recent work
397 has highlighted potential artefacts associated with microCT studies of embolism repair (Savi et
398 al., 2017; Petruzzellis et al., 2018). Exposure to high doses of X-ray radiation during image
399 acquisition has been observed to cause rapid cell death in some plant species. If mechanisms of
400 embolism repair involve living cells in the xylem, which seems most likely, there is clear
401 potential that X-rays may damage these living cells and inhibit refilling. Here, we eliminated
402 the potential for tissue damage from microCT scans by using cohorts of plants, with each
403 individual scanned once, rather than rescanning the same individuals many times during the
404 experiment. While we could not track the status of individual vessels using this approach, it did
405 allow us to assess the refilling mechanism by determining (a) differences in mean PLV values
406 between treatments, and (b) the presence or absence of partially refilled vessels in the scans of
407 recovering plants. Based on these observations, we concluded that no repair mechanism was
408 operating in *E. saligna* during recovery from drought stress.
409
410 Recovery of hydraulic capacity in the 6-month recovery treatment was achieved by growth of
411 new xylem tissue, rather than refilling of existing xylem. This finding is consistent with studies
412 that have tracked recovery in conifer species over long time periods (~11 weeks) using dye
413 staining techniques (Brodribb et al., 2010; Hammond et al., 2019). In the SD treatment, we
414 found that 50-98% of vessels were embolised due to water stress, while plants in the MD
415 treatment exhibited minimal embolism in the majority of replicates. Over the 6-month recovery
416 period, microCT visualisation revealed that a new ring of xylem had formed outside the older
417 xylem, in which the vast majority of vessels remained embolised. The newly formed xylem
418 contained low levels of embolism and was of equivalent cross-sectional area to the older xylem
419 (Fig. 4). These results demonstrate that recovery of xylem hydraulic capacity occurred via
420 growth of new xylem over a period of months, rather than by a refilling mechanism that repaired
421 embolisms on a shorter time scale. Recent studies have also suggested that embolism repair is

not a common mechanism of recovery in woody plants after moderate or severe drought (Clearwater and Clark, 2003; Brodribb et al., 2010; Knipfer et al., 2015a). The mechanism and rate of recovery observed in *E. saligna* has implications for our understanding of the overall 'cost' of xylem embolism to woody plants and for process-based models that simulate recovery of woody vegetation after drought.

Interestingly, in the MD and SD treatments, the proportion of embolised vessels increased after rewatering. Thus, despite recovery of Ψ_x, the proportion of embolised vessels was higher after 1-3 weeks of recovery. This surprising and counter-intuitive result suggests embolism may continue to spread through the xylem network even after drought stress has been relieved. One week after MD and rewatering, two individuals suffered almost complete canopy loss after initially appearing to have recovered water potential to pre-drought levels in 24 hours. Notably, these two individuals also suffered significantly higher PLV compared with the three other plants in the treatment block that maintained canopy. In the 3-week recovery time point, the higher mean PLV was driven primarily by one individual that never recovered Ψ_x, suggesting that it died as a result of the severe drought treatment. The high PLV observed for some individuals at 1- and 3-weeks after rewatering has important implications for our understanding of mortality and canopy dieback processes in the field. In some instances, trees exposed to severe drought die a long time after being released from drought stress by significant rainfall events (Mueller et al., 2005; Breshears et al., 2009; Gu et al., 2015; Matusick et al., 2016). This has been interpreted by some as evidence that water stress and hydraulic failure are not playing a significant role in mortality (Gu et al., 2015). However, the high level of embolism retained in stems post-drought, and the possibility that this can spread further within the xylem while canopy transpiration is recovering, suggests that hydraulic injury continues to play a major role in mortality processes even after plant water status has improved.

In terms of vulnerability to embolism, leaf turgor loss, and stomatal regulation during drought, *E. saligna* is sensitive to water stress relative to other *Eucalyptus* species (Bourne et al. 2017). Consistent with this, E_{plant} declined rapidly as a result of stomatal closure with the onset of drought stress in both SD and MD treatments. This decrease in E_{plant} occurred prior to embolism formation and is consistent with previous studies showing that stomatal closure is coordinated to protect the plant from catastrophic spread of embolism within the xylem (Cochard et al., 1996; Irvine et al., 1998; Bartlett et al., 2016; Martin-StPaul et al., 2017). In the MD treatment, E_{plant} recovered to approximately half of pre-treatment values 24 hrs after rewatering and

remained at this level for 2 weeks after rewatering, despite full recovery of plant water status within 24 hrs (Fig. 1). The post-drought reduction in E_{plant} relative to pre-drought values observed for the MD treatment was not associated with xylem hydraulic limitations in four of five individuals, since PLV remained low in these plants. However, it is notable that one individual never recovered E_{plant}; this plant had higher PLV and shed its canopy 1 week after rewatering commenced. The dynamics of recovery in the MD plants provides evidence that elevated levels of xylem embolism led to slower recovery of leaf gas exchange, consistent with previous studies (Resco et al., 2009; Brodribb et al., 2010; Skelton et al., 2017). In the absence of increased embolism, reduced transpiration rates after drought likely reflects enhanced water use efficiency, which is commonly observed after moderate drought treatments (Pou et al., 2008; Martorell et al., 2014).

The SD treatment induced high levels of stem embolism and complete canopy loss in the majority of individuals exposed to this level of drought stress (ca. -3.7 MPa), despite *E. saligna* possessing evergreen leaf phenology. It has been proposed that leaf shedding acts as a "hydraulic fuse" allowing plants to reduce canopy transpiration and the probability of runaway embolism in stem xylem (Tyree et al., 1993; Pineda-García et al., 2013; Hochberg et al., 2017). Leaf water potential may also have declined to more negative values than measured for stem water potential, leading to catastrophic embolism within the leaf and subsequent leaf mortality (Cardoso et al., 2020). In SD plants, E_{plant} recovered as plants re-foliated, making it difficult to assess the impact of hydraulic limitation in the stem xylem on the recovery of leaf gas exchange. However, transpiration rates normalised to leaf area (E_c) were lower than pre-treatment levels at 3-weeks post-rewatering, suggesting limitations to recovery caused by hydraulic dysfunction (Fig. S2). At 18 weeks after the SD treatment, E_c had recovered nearly to pre-treatment levels and remained unchanged at the 6-month recovery period. The long-term recovery in transpiration rates was associated with growth of new xylem, as seen in microCT visualisation (Figs. 3, 4 and 5).

CONCLUSIONS

The recovery of xylem hydraulic capacity after a severe drought treatment was generated by growth of new xylem tissue rather than refilling of embolised vessels. There was no evidence of embolism repair, regardless of drought treatment (moderate or severe) or time interval following rewatering. Over a recovery period of 6 months, plants exposed to severe drought stress recovered from complete canopy loss and very high levels of stem embolism. This is

consistent with the ecology of *Eucalyptus* species, which are well adapted to recover from extreme drought stress by re-sprouting from epicormic buds following canopy dieback. Hence, slow recovery from catastrophic levels of embolism by growth of new xylem tissue is the most likely mechanism for *Eucalyptus* species following severe drought. Overall, we require additional studies that address the impact of droughts of variable intensity and duration, and subsequent recovery periods, to determine whether xylem refilling is an important or common physiological process across woody species.

ACKNOWLEDGMENTS

We thank Dr. Daniel Hausermann, Dr. Chris Hall and Dr. Anton Maksimenko from the Australian Synchrotron Imaging and Medical Beamline (IMBL) for assisting with the micro-computed tomography and image rendering. We thank Dr Markus Nolf for assistance with whole plant transpiration measurements and Debora Corso for assistance during the experiments at the Australian Synchrotron.

524 **REFERENCES**

525 Bartlett MK, Klein T, Jansen S, Choat B, Sack L (2016) The correlations and sequence of
526 plant stomatal, hydraulic, and wilting responses to drought. Proceedings of the National
527 Academy of Sciences 113: 13098–13103
528 Borghetti M, Edwards WRN, Grace J, Jarvis PG, Raschi A (1991) The refilling of embolized
529 xylem in *Pinus sylvestris* L. Plant, Cell & Environment 14: 357–369
530 Bourne AE, Creek D, Peters JMR, Ellsworth DS, Choat B (2017) Species climate range
531 influences hydraulic and stomatal traits in Eucalyptus species. Annals of Botany 120:
532 123–133
533 Breshears DD, Myers OB, Meyer CW, Barnes FJ, Zou CB, Allen CD, McDowell NG,
534 Pockman WT (2009) Tree die-off in response to global change-type drought: mortality
535 insights from a decade of plant water potential measurements. Frontiers in Ecology and
536 the Environment 7: 185–189
537 Brodersen CR (2013) Visualizing wood anatomy in three dimensions with high-resolution X-
538 ray micro-tomography (μCT) – a review –. IAWA Journal 34: 408–424
539 Brodersen CR, McElrone AJ (2013) Maintenance of xylem network transport capacity: a
540 review of embolism repair in vascular plants. Frontiers in Plant Science. doi:
541 10.3389/fpls.2013.00108
542 Brodersen CR, McElrone AJ, Choat B, Matthews MA, Shackel KA (2010) The dynamics of
543 embolism repair in xylem: in vivo visualizations using high-resolution computed
544 tomography. Plant Physiology 154: 1088–1095
545 Brodribb TJ, Bowman DJMS, Nichols S, Delzon S, Burlett R (2010) Xylem function and
546 growth rate interact to determine recovery rates after exposure to extreme water deficit.
547 New Phytologist 188: 533–542
548 Canny MJ (1997) Vessel contents during transpiration—embolisms and refilling. American
549 Journal of Botany 84: 1223–1230
550 Cardoso AA, Batz TA, McAdam SAM (2020) Xylem embolism resistance determines leaf
551 mortality during drought in *Persea americana*. Plant Physiology 182: 547–554
552 Čermák J, Huzulák J, Penka M (1980) Water potential and sap flow rate in adult trees with
553 moist and dry soil as used for the assessment of root system depth. Biologia Plantarum
554 22: 34–41
555 Charrier G, Cochard H, Améglio T (2013) Evaluation of the impact of frost resistances on
556 potential altitudinal limit of trees. Tree Physiol 33: 891–902
557 Charrier G, Torres-Ruiz JM, Badel E, Burlett R, Choat B, Cochard H, Delmas CEL, Domec J-

558 C, Jansen S, King A, et al (2016) Evidence for hydraulic vulnerability segmentation and
559 lack of xylem refilling under tension. Plant Physiology 172: 1657–1668
560 Choat B, Badel E, Burlett R, Delzon S, Cochard H, Jansen S (2016) Noninvasive
561 measurement of vulnerability to drought-induced embolism by x-ray microtomography.
562 Plant Physiology 170: 273–282
563 Choat B, Brodersen CR, McElrone AJ (2015) Synchrotron X-ray microtomography of xylem
564 embolism in *Sequoia sempervirens* saplings during cycles of drought and recovery. New
565 Phytologist 205: 1095–1105
566 Choat B, Brodribb TJ, Brodersen CR, Duursma RA, López R, Medlyn BE (2018) Triggers of
567 tree mortality under drought. Nature 558: 531–539
568 Choat B, Drayton WM, Brodersen C, Mattthews MA, Shackel KA, Wada H, Mcelrone AJ
569 (2010) Measurement of vulnerability to water stress-induced cavitation in grapevine: a
570 comparison of four techniques applied to a long-vesseled species: Comparison of
571 vulnerability curve technique in grapevine. Plant, Cell & Environment 33: 1502–1512
572 Choat B, Jansen S, Brodribb TJ, Cochard H, Delzon S, Bhaskar R, Bucci SJ, Feild TS,
573 Gleason SM, Hacke UG, et al (2012) Global convergence in the vulnerability of forests to
574 drought. Nature 491: 752–755
575 Choat B, Nolf M, Lopez R, Peters JMR, Carins-Murphy MR, Creek D, Brodribb TJ (2019)
576 Non-invasive imaging shows no evidence of embolism repair after drought in tree species
577 of two genera. Tree Physiol 39: 113–121
578 Christensen-Dalsgaard KK, Tyree MT (2014) Frost fatigue and spring recovery of xylem
579 vessels in three diffuse-porous trees *in situ*: Frost fatigue in diffuse-porous trees. Plant,
580 Cell & Environment 37: 1074–1085
581 Clearwater MJ, Clark CJ (2003) In vivo magnetic resonance imaging of xylem vessel contents
582 in woody lianas. Plant, Cell & Environment 26: 1205–1214
583 Clearwater MJ, Goldstein G (2005) Embolism repair and long distance water transport. *In*
584 NM Holbrook, MA Zwieniecki, eds, Vascular transport in plants. Academic Press,
585 Burlington, pp 375–399
586 Cobb AR, Choat B, Holbrook NM (2007) Dynamics of freeze–thaw embolism in *Smilax*
587 *rotundifolia* (Smilacaceae). American Journal of Botany 94: 640–649
588 Cochard H, Bréda N, Granier A (1996) Whole tree hydraulic conductance and water loss
589 regulation in *Quercus* during drought: evidence for stomatal control of embolism?
590 Annales des Sciences Forestières 53: 197–206
591 David TS, Pinto CA, Nadezhdina N, Kurz-Besson C, Henriques MO, Quilhó T, Cermak J,

592 Chaves MM, Pereira JS, David JS (2013) Root functioning, tree water use and hydraulic
593 redistribution in *Quercus suber* trees: A modeling approach based on root sap flow.
594 Forest Ecology and Management 307: 136–146
595 Ewers FW, Ameglio T, Cochard H, Beaujard F, Martignac M, Vandame M, Bodet C, Cruiziat
596 P (2001) Seasonal variation in xylem pressure of walnut trees: root and stem pressures.
597 Tree Physiology 21: 1123–1132
598 Gauthey A, Peters JMR, Carins-Murphy MR, Rodriguez-Dominguez CM, Li X, Delzon S,
599 King A, López R, Medlyn BE, Tissue DT, et al (2020) Visual and hydraulic techniques
600 produce similar estimates of cavitation resistance in woody species. New Phytologist
601 228: 884–897
602 Gleason SM, Wiggans DR, Bliss CA, Young JS, Cooper M, Willi KR, Comas LH (2017)
603 Embolized stems recover overnight in *Zea mays*: the role of soil water, root pressure, and
604 nighttime transpiration. Front Plant Sci. doi: 10.3389/fpls.2017.00662
605 Gu L, Pallardy SG, Hosman KP, Sun Y (2015) Drought-influenced mortality of tree species
606 with different predawn leaf water dynamics in a decade-long study of a central US forest.
607 Biogeosciences 12: 2831–2845
608 Hacke UG, Sperry JS (2003) Limits to xylem refilling under negative pressure in *Laurus*
609 *nobilis* and *Acer negundo*. Plant, Cell and Environment 26: 303–311
610 Hammond WM, Yu K, Wilson LA, Will RE, Anderegg WRL, Adams HD (2019) Dead or
611 dying? Quantifying the point of no return from hydraulic failure in drought-induced tree
612 mortality. New Phytologist 223: 1834–1843
613 Hochberg U, Windt CW, Ponomarenko A, Zhang Y-J, Gersony J, Rockwell FE, Holbrook
614 NM (2017) Stomatal closure, basal leaf embolism, and shedding protect the hydraulic
615 integrity of grape stems. Plant Physiology 174: 764–775
616 Holbrook NM, Ahrens ET, Burns MJ, Zwieniecki MA (2001) In vivo observation of
617 cavitation and embolism repair using magnetic resonance imaging. Plant Physiology 126:
618 27–31
619 Holbrook NM, Zwieniecki MA (1999) Embolism repair and xylem tension: do we need a
620 miracle? 120: 4
621 Irvine J, Perks MP, Magnani F, Grace J (1998) The response of *Pinus sylvestris* to drought:
622 stomatal control of transpiration and hydraulic conductance. Tree Physiology 18: 393–
623 402
624 Jacobsen AL, Pratt RB (2012) No evidence for an open vessel effect in centrifuge-based
625 vulnerability curves of a long-vesselled liana (*Vitis vinifera*). New Phytologist 194: 982–

990
Johnson KM, Jordan GJ, Brodribb TJ (2018) Wheat leaves embolized by water stress do not recover function upon rewatering. Plant, Cell & Environment 41: 2704–2714
Klein T, Zeppel MJB, Anderegg WRL, Bloemen J, De Kauwe MG, Hudson P, Ruehr NK, Powell TL, von Arx G, Nardini A (2018) Xylem embolism refilling and resilience against drought-induced mortality in woody plants: processes and trade-offs. Ecological Research. doi: 10.1007/s11284-018-1588-y
Knipfer T, Brodersen CR, Zedan A, Kluepfel DA, McElrone AJ (2015a) Patterns of drought-induced embolism formation and spread in living walnut saplings visualized using X-ray microtomography. Tree Physiol 35: 744–755
Knipfer T, Eustis A, Brodersen C, Walker AM, Mcelrone AJ (2015b) Grapevine species from varied native habitats exhibit differences in embolism formation/repair associated with leaf gas exchange and root pressure: Contrasting response of wild grapevines to drought stress. Plant, Cell & Environment 38: 1503–1513
Lamarque LJ, Corso D, Torres-Ruiz JM, Badel E, Brodribb TJ, Burlett R, Charrier G, Choat B, Cochard H, Gambetta GA, et al (2018) An inconvenient truth about xylem resistance to embolism in the model species for refilling *Laurus nobilis* L. Annals of Forest Science 75: 88
Lens F, Tixier A, Cochard H, Sperry JS, Jansen S, Herbette S (2013) Embolism resistance as a key mechanism to understand adaptive plant strategies. Current Opinion in Plant Biology 16: 287–292
Li X, Delzon S, Torres-Ruiz J, Badel E, Burlett R, Cochard H, Jansen S, King A, Lamarque LJ, Lenoir N, et al (2020) Lack of vulnerability segmentation in four angiosperm tree species: evidence from direct X-ray microtomography observation. Annals of Forest Science. doi: 10.1007/s13595-020-00944-2
Martin-StPaul N, Delzon S, Cochard H (2017) Plant resistance to drought depends on timely stomatal closure. Ecology Letters 20: 1437–1447
Martorell S, Diaz-Espejo A, Medrano H, Ball MC, Choat B (2014) Rapid hydraulic recovery in *Eucalyptus pauciflora* after drought: linkages between stem hydraulics and leaf gas exchange. Plant, Cell & Environment 37: 617–626
Matusick G, Ruthrof KX, Fontaine JB, Hardy GESJ (2016) *Eucalyptus* forest shows low structural resistance and resilience to climate change-type drought. Journal of Vegetation Science 27: 493–503
Mayr S, Schmid P, Laur J, Rosner S, Charra-Vaskou K, Dämon B, Hacke UG (2014) Uptake

660 of Water via Branches Helps Timberline Conifers Refill Embolized Xylem in Late
661 Winter. Plant Physiology 164: 1731–1740
662 McCutchan H, Shackel KA. 1992. Stem-water potential as a sensitive indicator
663 of water stress in prune trees (*Prunus domestica* L. cv. French). Journal of the
664 American Society for Horticultural Science 117: 607–611.
665 Molyneux DE, Davies WJ (1983) Rooting pattern and water relations of three pasture grasses
666 growing in drying soil. Oecologia 58: 220–224
667 Mueller RC, Scudder CM, Porter ME, Trotter RT, Gehring CA, Whitham TG (2005)
668 Differential tree mortality in response to severe drought: evidence for long-term
669 vegetation shifts. Journal of Ecology 93: 1085–1093
670 Nardini A, Lo Gullo MA, Salleo S (2011) Refilling embolized xylem conduits: Is it a matter
671 of phloem unloading? Plant Science 180: 604–611
672 Nardini A, Salleo S, Raimondo F (2003) Changes in leaf hydraulic conductance correlate with
673 leaf vein embolism in *Cercis siliquastrum* L. Trees - Structure and Function 17: 529–534
674 Nolf M, Lopez R, Peters JMR, Flavel RJ, Koloadin LS, Young IM, Choat B (2017)
675 Visualization of xylem embolism by X-ray microtomography: a direct test against
676 hydraulic measurements. New Phytologist 214: 890–898
677 Paganin D, Mayo SC, Gureyev TE, Miller PR, Wilkins SW (2002) Simultaneous phase and
678 amplitude extraction from a single defocused image of a homogeneous object. Journal of
679 Microscopy 206: 33–40
680 Peters JMR, Gauthey A, Lopez R, Carins-Murphy MR, Brodribb TJ, Choat B (2020) Non-
681 invasive imaging reveals convergence in root and stem vulnerability to cavitation across
682 five tree species. Journal of Experimental Botany. doi: 10.1093/jxb/eraa381
683 Petruzzellis F, Pagliarani C, Savi T, Losso A, Cavalletto S, Tromba G, Dullin C, Bär A,
684 Ganthaler A, Miotto A, et al (2018) The pitfalls of in vivo imaging techniques: evidence
685 for cellular damage caused by synchrotron X-ray computed micro-tomography. New
686 Phytologist 220: 104–110
687 Pineda-García F, Paz H, Meinzer FC (2013) Drought resistance in early and late secondary
688 successional species from a tropical dry forest: the interplay between xylem resistance to
689 embolism, sapwood water storage and leaf shedding: Drought resistance of tropical dry
690 forest species. Plant, Cell & Environment 36: 405–418
691 Plavcová L, Jansen S (2015) The role of xylem parenchyma in the storage and utilization of
692 nonstructural carbohydrates. *In* U Hacke, ed, Functional and ecological xylem anatomy.
693 Springer International Publishing, Cham, pp 209–234

694 Pockman WT, Sperry JS (1997) Freezing-induced xylem cavitation and the northern limit of
695 Larrea tridentata. Oecologia 109: 19–27
696 Pou A, Flexas J, Alsina M del M, Bota J, Carambula C, Herralde FD, Galmés J, Lovisolo C,
697 Jiménez M, Ribas-Carbó M, et al (2008) Adjustments of water use efficiency by stomatal
698 regulation during drought and recovery in the drought-adapted *Vitis* hybrid Richter-110
699 (*V. berlandieri* × *V. rupestris*). Physiologia Plantarum 134: 313–323
700 R Core Team (2017) R: A language and environment for statistical computing. R Foundation
701 for Statistical Computing, Vienna, Austria. URL https://www.R-project.org/.
702 Rehschuh R, Cecilia A, Zuber M, Faragó T, Baumbach T, Hartmann H, Jansen S, Mayr S,
703 Ruehr N (2020) Drought-induced xylem embolism limits the recovery of leaf gas
704 exchange in scots pine. Plant Physiology 184: 852–864
705 Resco V, Ewers BE, Sun W, Huxman TE, Weltzin JF, Williams DG (2009) Drought-induced
706 hydraulic limitations constrain leaf gas exchange recovery after precipitation pulses in the
707 C3 woody legume, Prosopis velutina. New Phytologist 181: 672–682
708 Robichaux RH, Grace J, Rundel PW, Ehleringer JR (1987) Plant water balance. BioScience
709 37: 30–37
710 RStudio Team (2015) RStudio: Integrated Development for R. RStudio, Inc., Boston, MA
711 URL http://www.rstudio.com/.
712 Ryu J, Hwang BG, Lee SJ (2016) In vivo dynamic analysis of water refilling in embolized
713 xylem vessels of intact *Zea mays* leaves. Ann Bot 118: 1033–1042
714 Salleo S, Gullo MAL, Paoli D, Zippo M (1996) Xylem recovery from cavitation-induced
715 embolism in young plants of *Laurus nobilis*: a possible mechanism. New Phytologist
716 132: 47–56
717 Salleo S, Trifilò P, Esposito S, Nardini A, Gullo MAL (2009) Starch-to-sugar conversion in
718 wood parenchyma of field-growing *Laurus nobilis* plants: a component of the signal
719 pathway for embolism repair? Functional Plant Biol 36: 815–825
720 Savi T, Miotto A, Petruzzellis F, Losso A, Pacilè S, Tromba G, Mayr S, Nardini A (2017)
721 Drought-induced embolism in stems of sunflower: A comparison of in vivo micro-CT
722 observations and destructive hydraulic measurements. Plant Physiology and
723 Biochemistry 120: 24–29
724 Scholander PF, Hammel HT, Bradstreet ED, Hemmingsen EA (1965) Sap pressure in
725 vascular plants. Science 148: 339–346
726 Secchi F, Pagliarani C, Cavalletto S, Petruzzellis F, Tonel G, Savi T, Tromba G, Obertino
727 MM, Lovisolo C, Nardini A, et al (2020) Chemical inhibition of xylem cellular activity

728 impedes the removal of drought-induced embolisms in poplar stems – new insights from
729 micro-CT analysis. New Phytologist. doi: https://doi.org/10.1111/nph.16912
730 Skelton RP, Brodribb TJ, McAdam SAM, Mitchell PJ (2017) Gas exchange recovery
731 following natural drought is rapid unless limited by loss of leaf hydraulic conductance:
732 evidence from an evergreen woodland. New Phytologist 215: 1399–1412
733 Sperry JS, Donnelly JR, Tyree MT (1988) Seasonal Occurrence of Xylem Embolism in Sugar
734 Maple (Acer saccharum). American Journal of Botany 75: 1212–1218
735 Sperry JS, Holbrook NM, Zimmermann MH, Tyree MT (1987) Spring filling of xylem
736 vessels in wild grapevine. Plant Physiology 83: 414–417
737 Steudle E (2001) The Cohesion-Tension Mechanism and the Acquisition of Water by Plant
738 Roots. Annual Review of Plant Physiology and Plant Molecular Biology 52: 847–875
739 Taneda H, Sperry JS (2008) A case-study of water transport in co-occurring ring- versus
740 diffuse-porous trees: contrasts in water-status, conducting capacity, cavitation and vessel
741 refilling. Tree Physiology 28: 1641–1651
742 Torres-Ruiz JM, Jansen S, Choat B, McElrone AJ, Cochard H, Brodribb TJ, Badel E, Burlett
743 R, Bouche PS, Brodersen CR, et al (2015) Direct X-Ray microtomography observation
744 confirms the induction of embolism upon xylem cutting under tension. Plant Physiology
745 167: 40–43
746 Tyree MT (1997) The Cohesion-Tension theory of sap ascent: current controversies. J Exp
747 Bot 48: 1753–1765
748 Tyree MT, Cochard H, Cruiziat P, Sinclair B, Ameglio T (1993) Drought-induced leaf
749 shedding in walnut: evidence for vulnerability segmentation. Plant, Cell & Environment
750 16: 879–882
751 Tyree MT, Ewers FW (1991) The hydraulic architecture of trees and other woody plants. New
752 Phytologist 119: 345–360
753 Tyree MT, Salleo S, Nardini A, Assunta Lo Gullo M, Mosca R (1999) Refilling of embolized
754 vessels in young stems of laurel. Do we need a new paradigm? Plant Physiology 120: 11–
755 22
756 Utsumi Y, Sano Y, Fujikawa S, Funada R, Ohtani J (1998) Visualization of cavitated vessels
757 in winter and refilled vessels in spring in diffuse-porous trees by cryo-scanning electron
758 microscopy. Plant Physiology 117: 1463–1471
759 Wheeler JK, Huggett BA, Tofte AN, Rockwell FE, Holbrook NM (2013) Cutting xylem
760 under tension or supersaturated with gas can generate PLC and the appearance of rapid
761 recovery from embolism: Sampling induced embolism. Plant, Cell & Environment 36:

1938–1949
Yang S-J, Zhang Y-J, Sun M, Goldstein G, Cao K-F (2012) Recovery of diurnal depression of leaf hydraulic conductance in a subtropical woody bamboo species: embolism refilling by nocturnal root pressure. Tree Physiology 32: 414–422
Zwieniecki MA, Holbrook NM (2009) Confronting Maxwell's demon: biophysics of xylem embolism repair. Trends in Plant Science 14: 530–534

FIGURE LEGENDS

Figure 1. Changes in water potential (Ψ_x, -MPa) and whole plant transpiration rate (E_{plant}; g plant^{-1} h^{-1}) during drought and recovery for two drought treatments: moderate drought (A) and (C) blue symbols, and severe drought (B) and (D) (magenta symbols). Grey symbols show individual data points. Measurement time points shown on the x-axis are well-watered (WW), moderate drought (MD), severe drought (SD), 24 hrs after rewatering (R24h), 5 days after rewatering (R5d), 1 week after rewatering (R1wk), 2 weeks after rewatering (R2wk), 3 weeks after rewatering (R3wk), 18 weeks after rewatering (R18wk), and 6 months rewatering (R6mo). Letters indicate significant differences between time point within each treatment based on Tukey HSD test at a=0.05).

Figure 2. Percent loss of vessels (PLV) to embolism at different time points during drought and recovery for two treatments (A. medium drought, blue; B. severe drought, magenta). Grey symbols show individual data points. Measurement time points shown on the x-axis are well-watered (WW), moderate drought (MD), severe drought (SD), 24 hrs after rewatering (R24h), 1 week after rewatering (R1wk), 3 weeks after rewatering (R3wk), and 6 months rewatering (R6mo). For the 6-month recovery point after severe drought, PLV is shown for the total stem cross-section (magenta) and for the new ring of xylem (purple). Letters indicate significant differences between time point within each treatment based on Tukey HSD test at a=0.05).

Figure 3. Transverse slices from microCT scans of *Eucalyptus saligna* at different time points during drought and recovery. At left, well-watered (WW) treatment. In blue (upper), moderate drought treatment (MD), recovery at 24 hours (R24h) and recovery at 1 week (R1wk). In magenta (lower), severe drought treatment (SD), recovery at 3 weeks (R3wk), recovery at 6-months (R6mo). Xylem vessels that have become embolised are highlighted in red. The corresponding water potential and PLV are indicated on each image. For the recovery treatment, Ψ_{min} corresponds to the most negative water potential reached by the plant before rewatering. For R6mo, PLV_{tot} is the PLV of the entire cross section and PLV_{NX} is the PLV measured in the new xylem formed during recovery.

Figure 4. (A) Transverse slice from microCT scan of *Eucalyptus saligna* plant after 6 months of recovery from severe drought stress. The xylem area exposed to the severe drought treatment (old xylem; orange arrow) contains a very high proportion embolised vessels. The new ring of

xylem (new xylem; green arrow) formed subsequent to the severe drought stress treatment during 6-month recovery period contains a much lower proportion of embolised vessels. (B) Box plot showing the percentage of total xylem area occupied by the new growth formed during recovery period.

Figure 6. Percentage loss of vessels (PLV) as a function of stem water potential (Ψ_x, -MPa) for *Eucalyptus saligna* plants exposed to drought and recovery treatments. Each data point represents one individual from dehydration treatment (yellow symbols) or recovery treatment (purple symbols) including individuals for 24 hrs, 1 week or 3 weeks after rewatering. For recovery plants, data were also plotted for the minimum water potential reached by each individual before rewatering (transposition; triangles). Curves were fit to drought and transposition groups using a Weibull function. The vertical solid lines indicate the Y_x at which 50% of vessels become embolized (P_{50}) for dehydration and transposition curves with dashed lines showing the 95% confidence intervals around estimates of P_{50}.

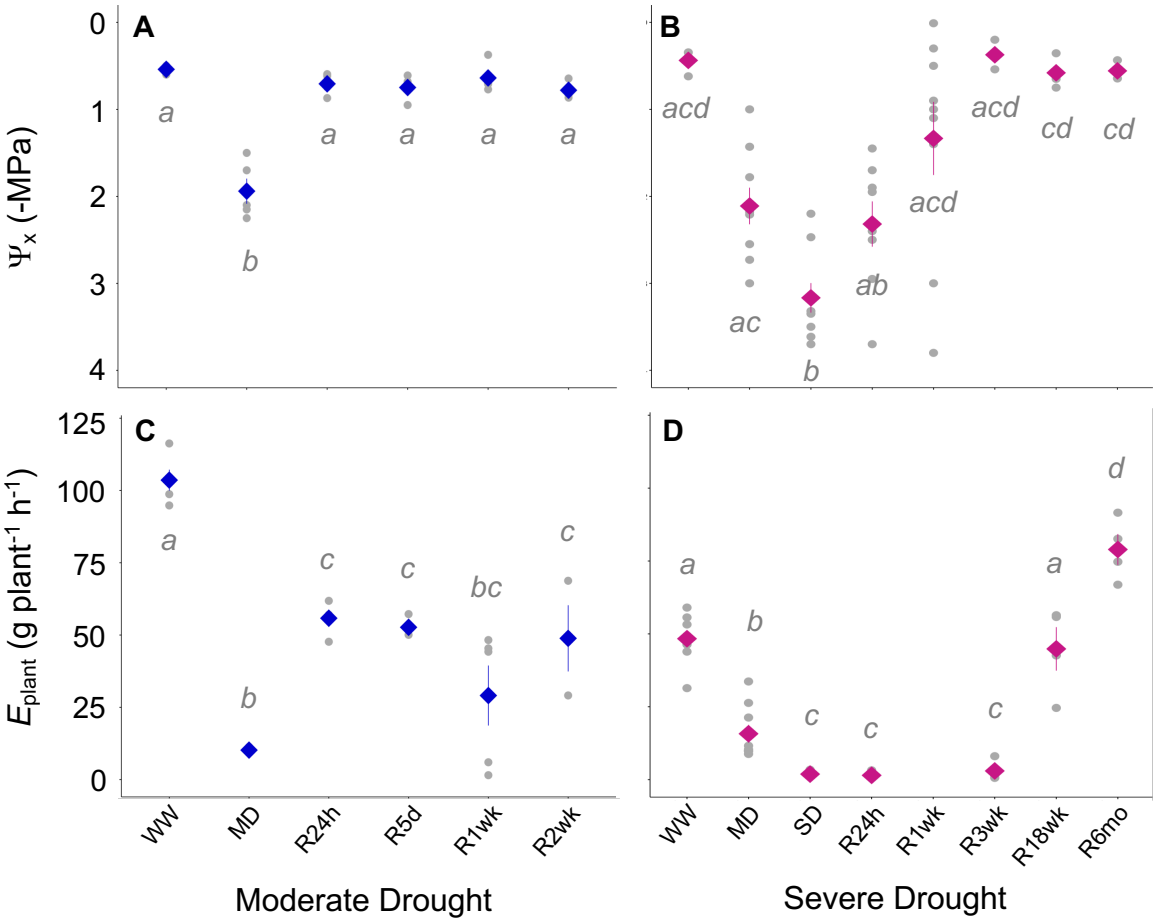

Figure 1. Changes in water potential (Ψ_x, -MPa) and whole plant transpiration rate (E_{plant}; g plant^{-1} h^{-1}) during drought and recovery for two drought treatments: moderate drought (A) and (C) blue symbols, and severe drought (B) and (D) (magenta symbols). Grey symbols show individual data points. Measurement time points shown on the x-axis are well-watered (WW), moderate drought (MD), severe drought (SD), 24 hrs after rewatering (R24h), 5 days after rewatering (R5d), 1 week after rewatering (R1wk), 2 weeks after rewatering (R2wk), 3 weeks after rewatering (R3wk), 18 weeks after rewatering (R18wk), and 6 months rewatering (R6mo). Letters indicate significant differences between time point within each treatment based on Tukey HSD test at α=0.05).

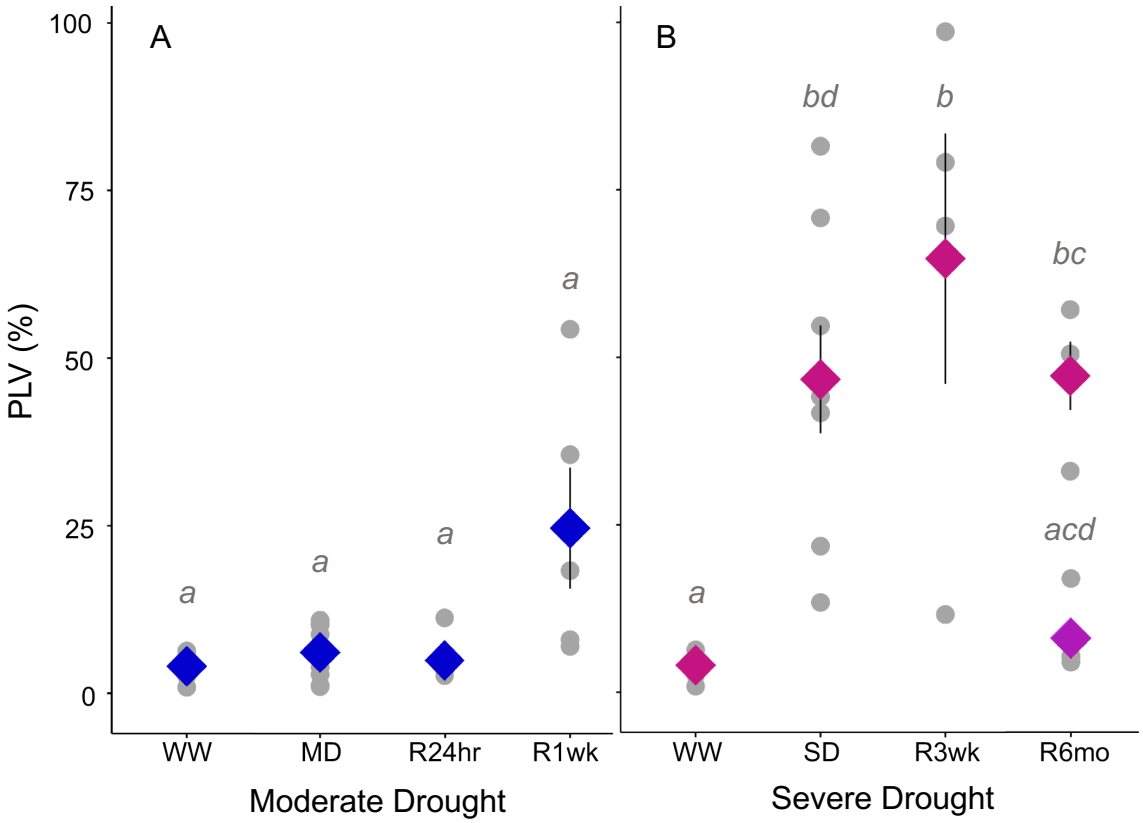

Figure 2. Percent loss of vessels (PLV) to embolism at different time points during drought and recovery for two treatments (A. moderate drought, blue; B. severe drought, magenta). Grey symbols show individual data points. Measurement time points shown on the x-axis are well-watered (WW), moderate drought (MD), severe drought (SD), 24 hrs after rewatering (R24h), 1 week after rewatering (R1wk), 3 weeks after rewatering (R3wk), and 6 months rewatering (R6mo). For the 6-month recovery point after severe drought, PLV is shown for the total stem cross-section (magenta) and for the new ring of xylem (purple). Letters indicate significant differences between time point within each treatment based on Tukey HSD test at α=0.05).

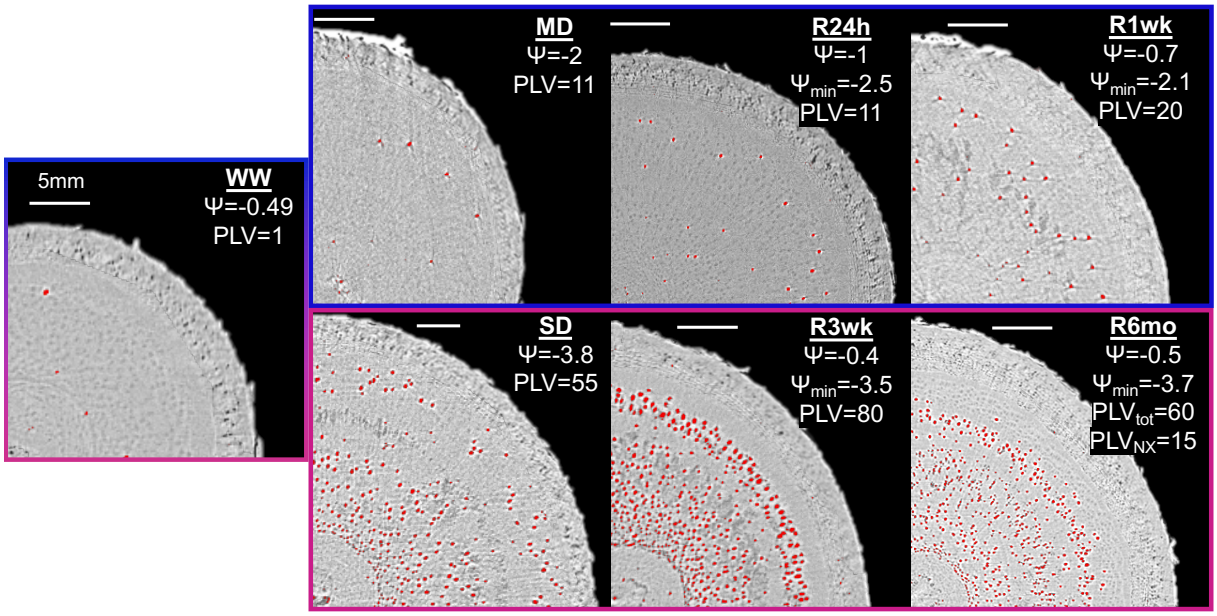

Figure 3. Transverse slices from microCT scans of *Eucalyptus saligna* at different time points during drought and recovery. At left, well-watered (WW) treatment. In blue (upper), moderate drought treatment (MD), recovery at 24 hours (R24h) and recovery at 1 week (R1wk). In magenta (lower), severe drought treatment (SD), recovery at 3 weeks (R3wk), recovery at 6-months (R6mo). Xylem vessels that have become embolised are highlighted in red. The corresponding water potential and PLV are indicated on each image. For the recovery treatment, Ψ_{min} corresponds to the most negative water potential reached by the plant before rewatering. For R6mo, PLV_{tot} is the PLV of the entire cross section and PLV_{NX} is the PLV measured in the new xylem formed during recovery.

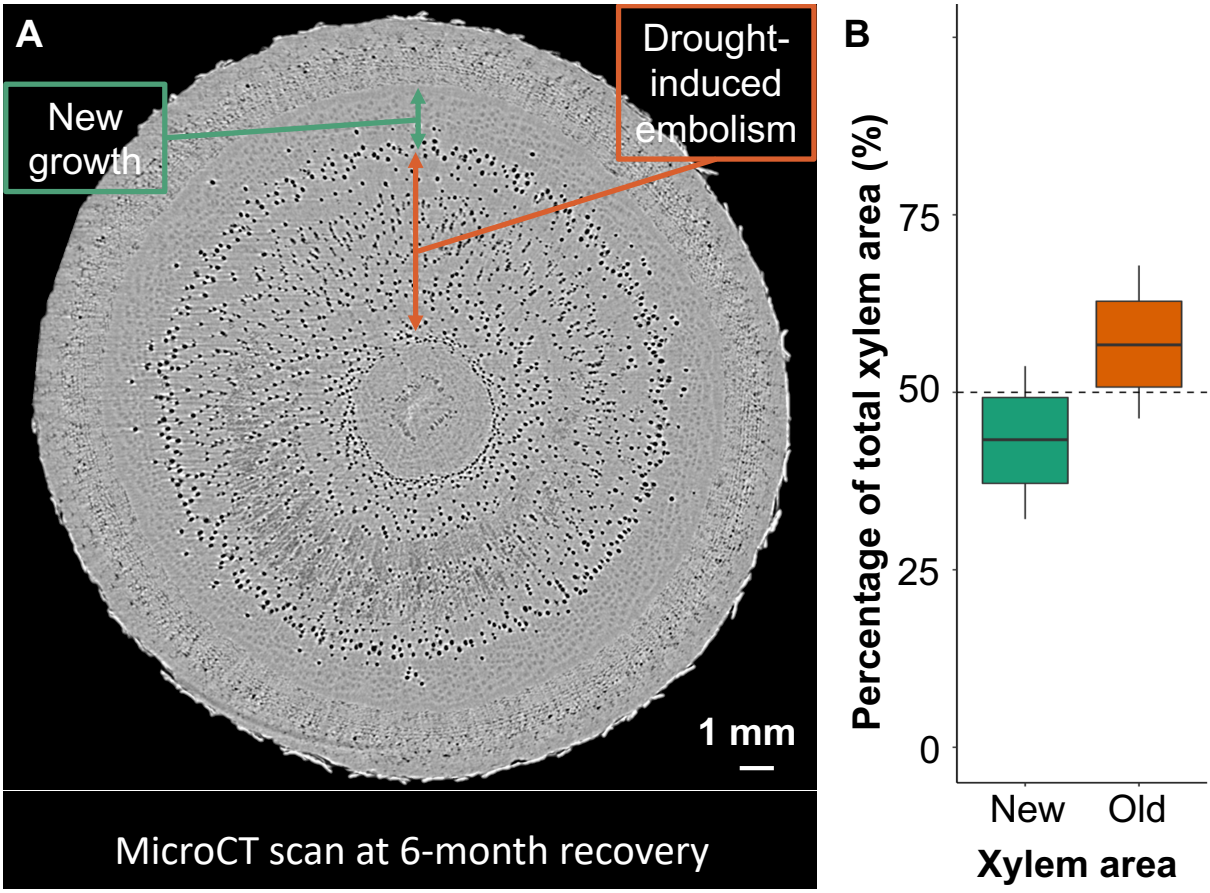

Figure 4. (A) Transverse slice from microCT scan of *Eucalyptus saligna* plant after 6 months of recovery from severe drought stress. The xylem area exposed to the severe drought treatment (old xylem; orange arrow) contains a very high proportion embolised vessels. The new ring of xylem (new xylem; green arrow) formed subsequent to the severe drought stress treatment during 6-month recovery period contains a much lower proportion of embolised vessels. (B) Box plot showing the percentage of total xylem area occupied by the new growth formed during recovery period.

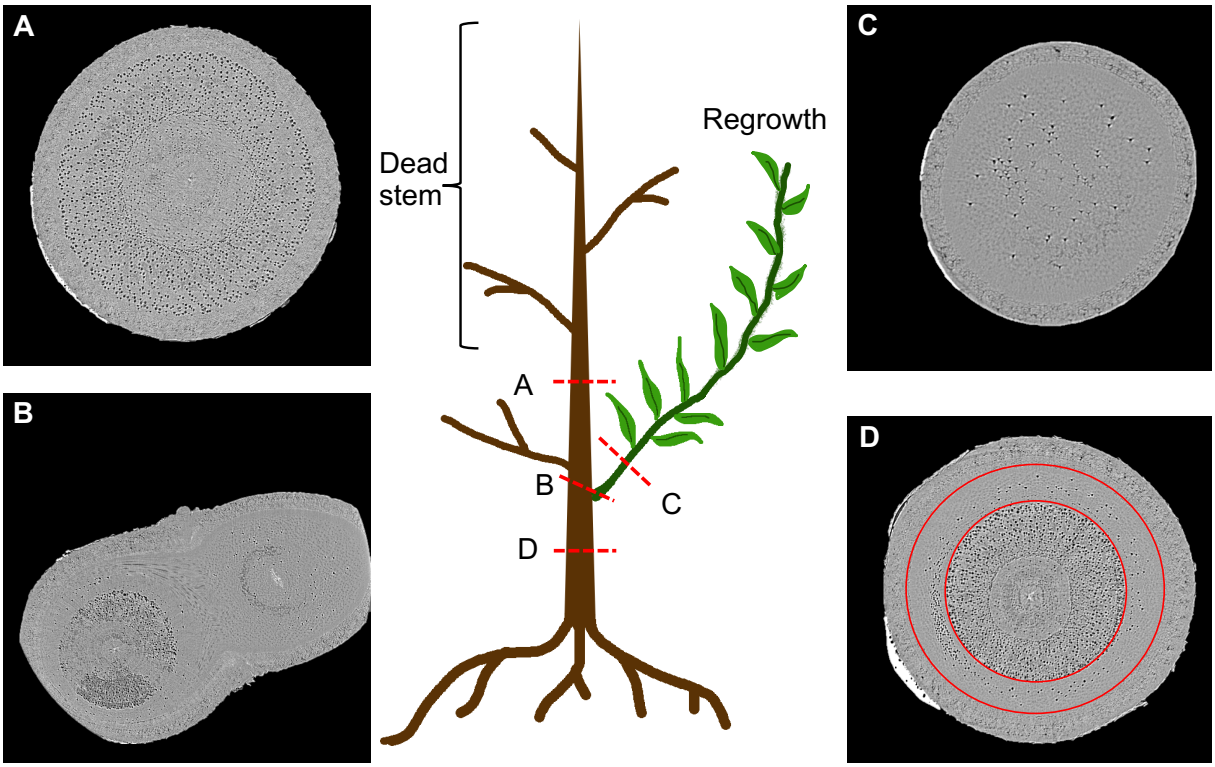

Figure 5. Transverse slices from microCT scans along the stem axis of one *Eucalyptus saligna* individual at the 6-month recovery time point. In this individual, the majority of the main stem axis died after a severe drought treatment and a lateral shoot became the new leader after rewatering. Scans taken at different points on the stem axis show occurrence of embolism in this plant. (A) Dead upper stem with all vessels embolised; (B) slice capturing the branching point between the main stem axis and the new leader; (C) slice showing new leader with scattered embolized vessels; (D) stem base with inner ring of embolized vessels exposed to severe drought and new ring of xylem grown during the 6-month recovery period (shown in red).

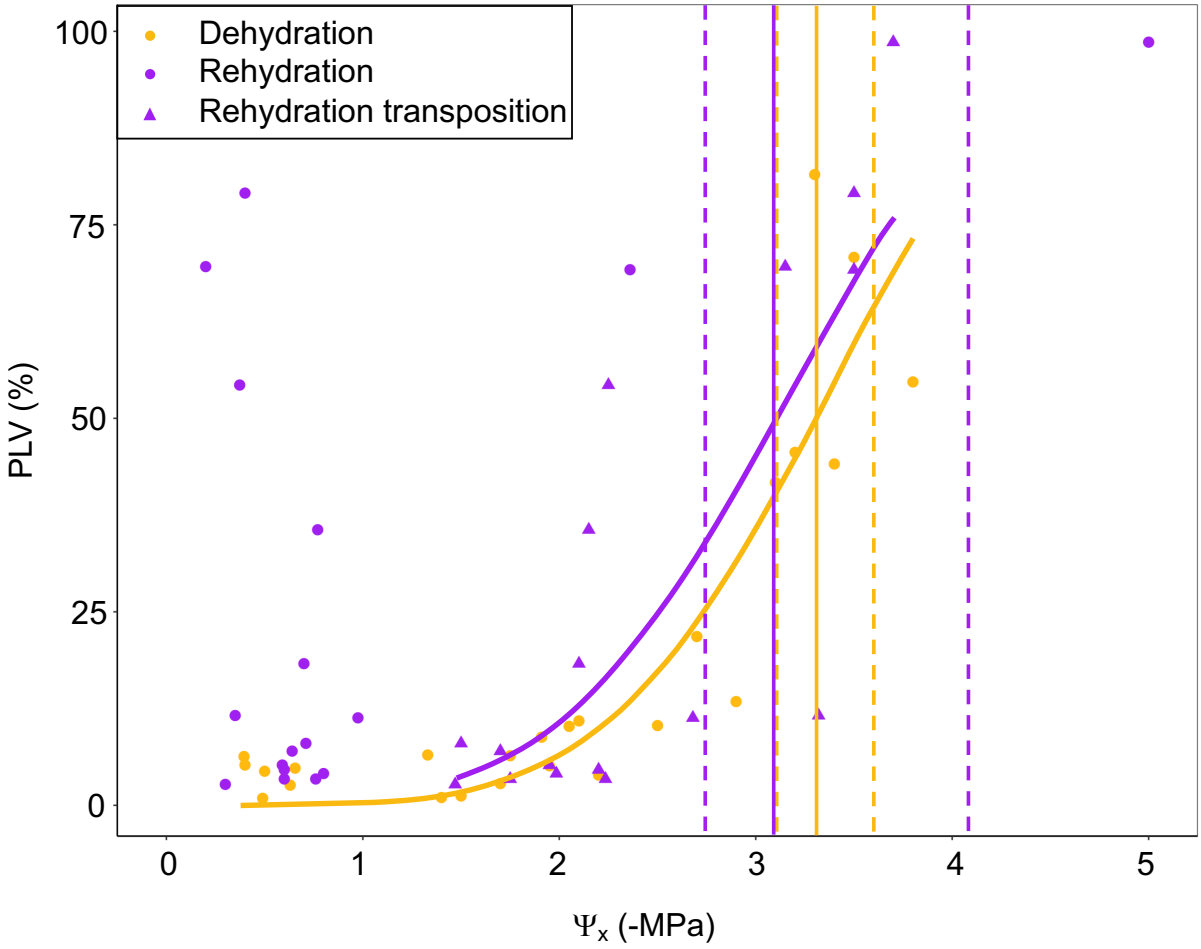

Figure 6. Percentage loss of vessels (PLV) as a function of stem water potential (Ψ_x, -MPa) for *Eucalyptus saligna* plants exposed to drought and recovery treatments. Each data point represents one individual from dehydration treatment (yellow symbols) or recovery treatment (purple symbols) including individuals for 24 hrs, 1 week or 3 weeks after rewatering. For recovery plants, data were also plotted for the minimum water potential reached by each individual before rewatering (transposition; triangles). Curves were fit to drought and transposition groups using a Weibull function. The vertical solid lines indicate the Ψ_x at which 50% of vessels become embolized (P_{50}) for dehydration and transposition curves with dashed lines showing the 95% confidence intervals around estimates of P_{50}.

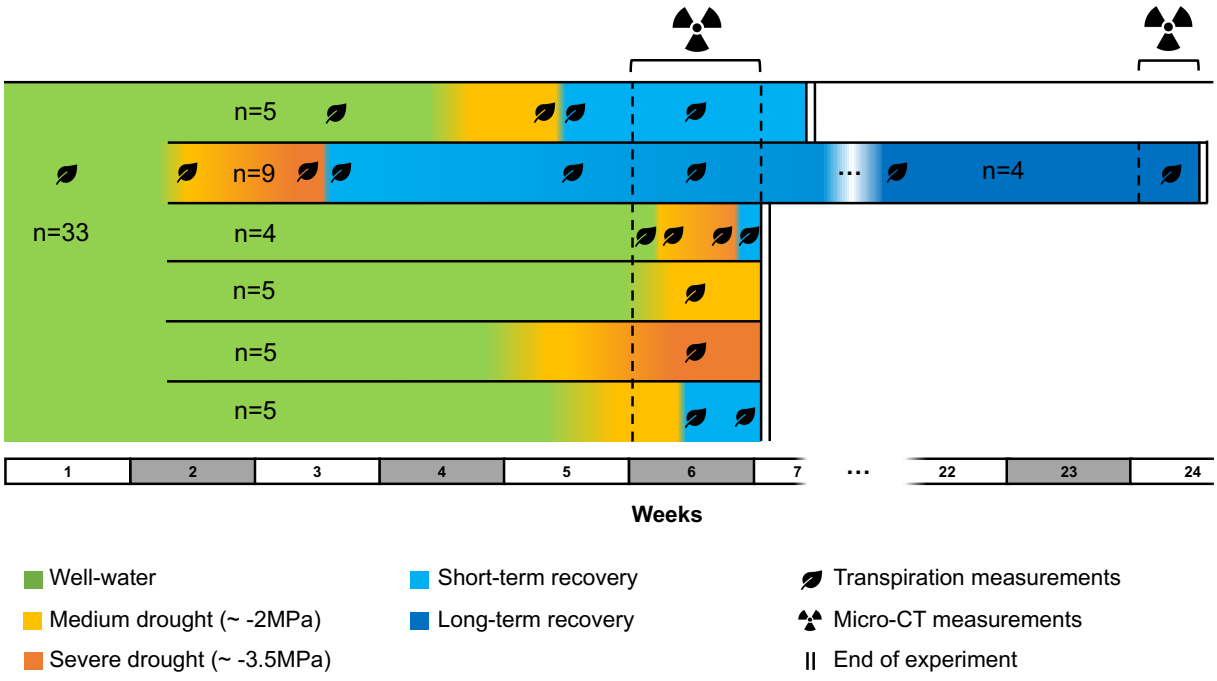

Figure S1. Experimental timeline for treatment groups including the timing of transpiration measurements and microCT scans. Colours indicate the water status of plants during the proregression of treatments.

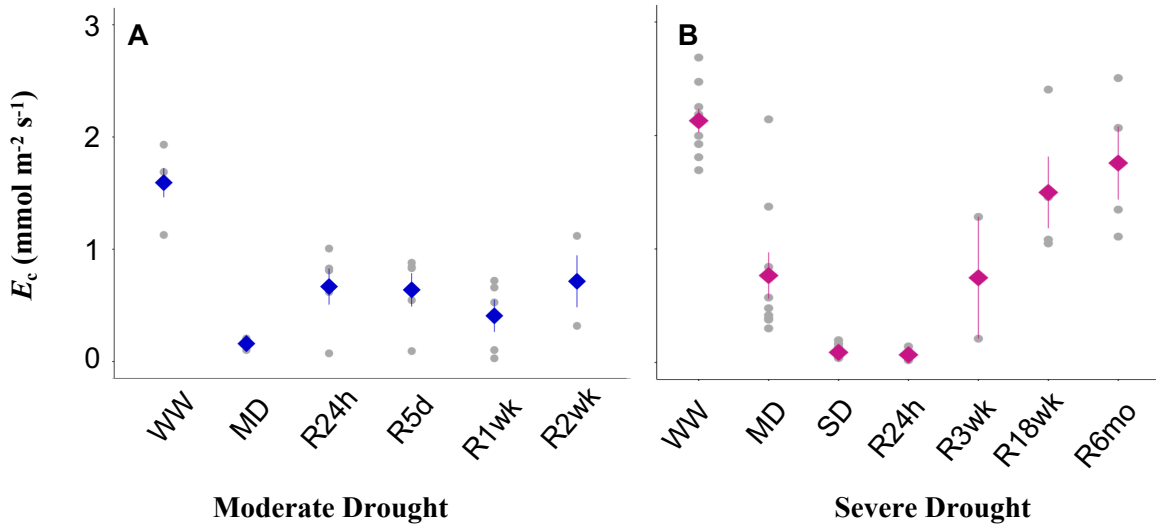

Figure S2. Changes in whole plant transpiration rate as a function of leaf area (E_c; mmol m^{-2} s^{-1}) during drought and recovery for two drought treatments: moderate drought (A; blue symbols) and severe drought (B; magenta symbols). Grey symbols show individual data points. Measurement time points shown on the x-axis are well-watered (WW), moderate drought (MD), severe drought (SD), 24 hrs after rewatering (R24h), 5 days after rewatering (R5d), 1 week after rewatering (R1wk), 2 weeks after rewatering (R2wk), 3 weeks after rewatering (R3wk), 18 weeks after rewatering (R18wk), and 6 months rewatering (R6mo).